# Broadband Emission of GaAs/AlGaAs Quantum-Well Superluminescent Diode at 850 nm

C. E. Dimas, C. T. Vishton, R. A. Merola, H. S. Djie, and B. S. Ooi*
Center for Optical Technologies and Electrical and Computer Engineering Department
Lehigh University, Bethlehem, PA 18015, USA

## ABSTRACT

We report the fabrication and characterization of broad emission linewidth GaAs/AlGaAs quantum-well based superluminescent diodes. A photon absorption section and an optical amplifier sections are monolithically integrated on the device to suppress feedback oscillation and to amplifier the optical power, respectively. The device emitters at 850 nm peak wavelength, and exhibits a broad bandwidth of 65 nm, output power > 3.5 mW, and a spectral ripple of 0.5 dB at 20ºC under continuous wave operation.

**Keywords:** Superluminescent diode, optical coherence tomography, quantum-well, GaAs/AlGaAs laser.

## 1. INTRODUCTION

The need for high performance superluminescent diodes (SLDs) stems from the increasing use of broadband light sources in a variety of sensing and imaging applications, including optical coherence tomography (OCT). Based on the low coherence interferometry principle, OCT technology has enabled many non-invasive, high volume tissue imaging applications such as retinal imaging with 10-100 times greater depth resolution than ultrasound technology [1]. The coherence length defines the axial resolution of the OCT system, which is inversely proportional to the spectral width of the light source. In order to continue to improve the depth resolution, light sources with broader spectral widths are needed. The optical power and the peak wavelength of the light source determine the signal to noise ratio and the imaging depth of the OCT system. A peak emission wavelength about 850 nm is typically employed for retinal imaging applications, as the absorption of ocular fundus is at a minimum in this wavelength range [2], [3].

An SLD has advantages over other broadband light sources such as batch fabrication using mature semiconductor processing, high efficiency, Gaussian-like spectrum, and compact size. Various approaches for various wavelength regimes have been implemented to enhance the SLD bandwidth including asymmetric quantum-well (QW) configurations [4], inhomogeneous quantum-dot or dash structures [5,6], selective area epitaxy [7], and quantum well intermixing [8]. In early work, Semenov et al. have demonstrated the utilization of amplified spontaneous emission from several quantized levels in asymmetric QW's [9]. The device was simultaneously pumped with the combination of continuous wave (CW) and pulse-mode currents to avoid thermal roll-off under high current injection and achieve broadband emission. However, this composite current injection scheme is not practical for many applications. Another approach implemented a single QW active region and multi-electrode pumping to achieve broad spectrums [10]. However, broadening the spectrum results in a non-Gaussian-like emission. Although high emission power can be accomplished by using multimode SLD device designs [11], single lateral mode emission remains important for efficient device to fiber coupling and greater sensitivity applications that require lowest loss, broader bandwidth and lowest dispersion. Therefore we address the need for a single mode, CW driven SLD with broad Gaussian-like spectrum.

In this work, we report the design, fabrication, and characterization of a GaAs/AlGaAs double QW SLD emitting at ~850 nm. The device consists of three sections: a photon absorber (PA), an emitter section ($D_1$), and an optical amplifier ($D_2$) as schematically illustrated in Fig. 1. The photon absorber and anti-reflection (AR) coating (1%-2%) were used to restrain the Fabry-Perot oscillations from the emitter and rear facets respectively. The $D_2$ section is pumped to transparent for optical amplification.

*bsooi@lehigh.edu; phone 1 610 758 2606; fax 1 610 758 2605; www.ece.lehigh.edu/~bsooi

Integrated Optics: Devices, Materials, and Technologies XI, edited by Yakov Sidorin, Christoph A. Waechter,
Proc. of SPIE Vol. 6475, 64751B, (2007) · 0277-786X/07/$18 · doi: 10.1117/12.700747

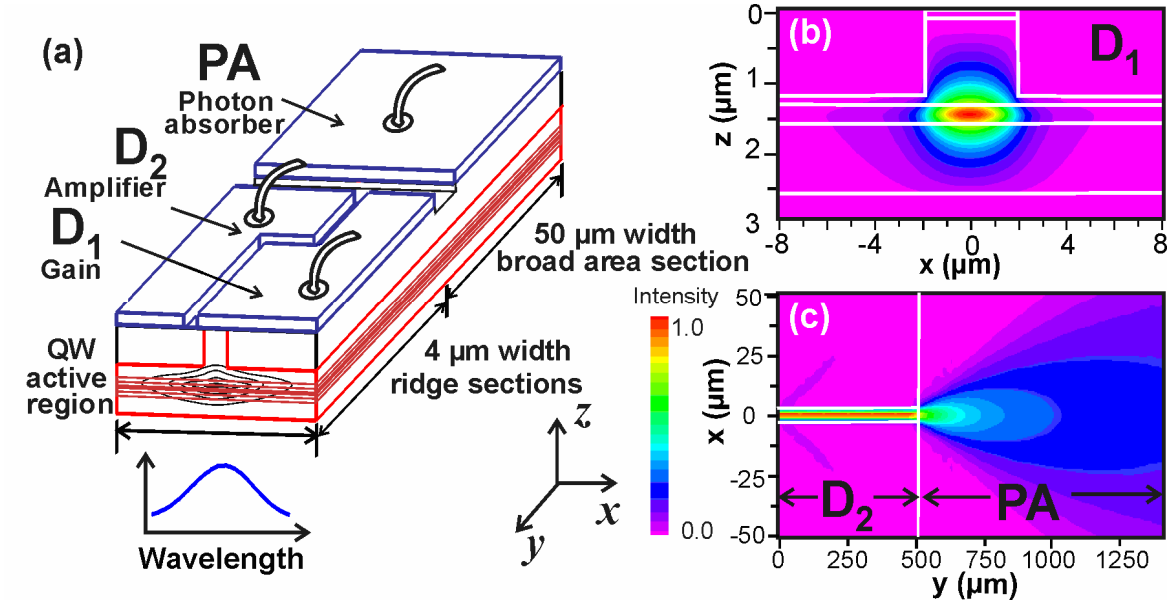


Fig. 1. (a) The schematic device structure of three-section QW SLD consisting of two 4 μm wide ridge waveguide active sections ($D_1$ and $D_2$) and an integrated 50 μm wide broad area photon absorber (PA). (b) The simulated cross section of the optical confinement in the ridge waveguide $D_1$ and $D_2$. (c) The simulated light spreading along the longitudinal direction y from $D_2$ to PA.

## 2. DEVICE AND WAFER STRUCTURE DESIGNS

The wafer structure consisted of a double QW active region designed to emit a center wavelength at 850 nm. The wafer was grown by metal-organic vapor phase epitaxy (MOVPE) on a GaAs substrate. The active region consists of two 10 nm wide GaAs QWs, separated by an undoped 10 nm $Al_{0.2}Ga_{0.8}As$ barrier, and based on a separate confinement heterostructure configuration. Both the upper and lower cladding $Al_{0.4}Ga_{0.6}As$ layers are 1.5 μm thick and doped at a concentration of $5x10^{17}$ $cm^{-3}$ using Zn and Si respectively. The top contact epitaxial layer is a 0.1 μm GaAs layer doped with Zn at $5x10^{18}$ $cm^{-3}$.

The SLD device fabrication followed the standard ridge-waveguide fabrication process. First, the inter-electrode separation was defined by removing the highly doped contact layer using selective chemical etching. Plasma etching using Cl-based gasses formed 1.1 μm deep ridge sections. A 200 nm thick $SiO_2$ layer, deposited using plasma enhanced chemical vapor deposition method, was patterned and wet etched to open the electrode contacts. The final steps of the fabrication involved p-contact evaporation (Ti/Pt/Au) and metal lift-off to define electrodes, substrate thinning, n-contact (Au/Ge/Au/Ni/Au) evaporation, and annealing for metal alloying. Anti-reflection (AR) coating, comprised of a multi-layer of $ZrO/SiO_2$, was applied on the emitter facet to further suppress the feedback oscillation.

The device design consisted of a multi-electrode configuration. The $D_1$ and $D_2$ sections are 4 μm wide, 1.1 μm deep weakly guided ridge waveguides, for single lateral mode operation. The PA section is in the form of a 50 μm wide broad area slab-guide to prevent optical feedback and suppress lasing action. Another important aspect of the device design is the multi-electrode configuration with electrically isolated regions at the butt-coupling interface. This isolation resistance of > 100 Ohms is much greater than the voltage to current ratio of any of the diodes ($D_1$, $D_2$, and PA). Such resistance is sufficient to electrically isolate the electrodes. We can model this isolation region as a pure resistance, since the voltage over this region (i.e. $V_{D1}$-$V_{D2}$) is 97% linear with respect to the injection current to the $D_1$ section. The leakage in between the electrodes of ~1% does not affect the overall electrical characteristic of the device. The main benefit of the multi-electrode configuration is the flexibility to drive both $D_1$ and $D_2$ separately or together. The electrode lengths of the PA and $D_2$ sections are 500 μm and 270 μm respectively. The length of the $D_1$ section varies from 500 μm to 1000 μm for characterization. These devices were mounted p-side up on a temperature-controlled heatsink and characterized under CW operation at 20ºC.

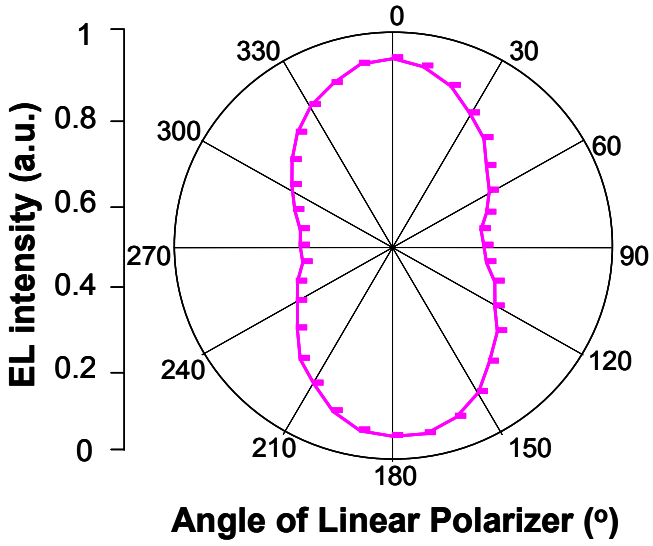


Fig. 2. Normalized optical power at various angle of rotation of a polarizer. The emission is thus characterized as being elliptically polarized TE/TM 2:1.

Measurements of optical power were taken to quantify the polarization state by launching the output light through a rotating linear polarizer. The SLD emission was observed to be elliptically polarized with an optical power ratio of TE/TM polarization is 2:1 as depicted in Figure 3.

## 3. RESULTS AND DISCUSSIONS

The optimum devices found had the following two sets of specifications: (1) AR coating on the emitter side with $D_1$ 500 μm in length, and (2) AR coating on both the emitter and absorber facet with $D_1$ 850 μm in length. Devices with a longer length of $D_1$ (850 μm) resulted in greater power at the expense of reduced bandwidth. In both device sets, a single CW injection current to $D_1$ proved optimal for gain amplification and the simultaneous excitation of confined states in the QW [9].

### 3.1 SLDs with $D_1$ at 500 μm Length

Figure 4 shows the light-current (L-I) characteristics of the SLD with $D_1$ 500 μm in length, before and after the application of AR coating to the emitter facet. The $D_1$ section was driven with CW current, while the $D_2$ and PA sections were floating. The device without AR coating exhibits lasing action at a relatively low current of 60 mA. With AR coating applied, the lasing action can be effectively suppressed and the L-I characteristics gives as expected a linear behavior with increasing current injection. A maximum output power of greater than 3.5 mW is obtained at a total current injection of 200 mA. At injection currents above 200 mA, thermal roll off begins to appear, primarily due to the overheating in the gain section. The inset in Figure 4 presents the corresponding electroluminescent spectrum, centered at 850 nm, from SLDs with and without AR coating. The maximum spontaneous emission of the SLD without AR coating yields only 0.8 mW of power with a full-with-half-maximum (FWHM) of 33 nm and a spectral ripple of 0.6 dB. The spectrum modulation is measured at the center wavelength within a 10 nm span with an optical spectrum analyzer with 0.05 nm resolution. The AR-coated SLD produces a nearly flattop emission with a FWHM of 65 nm and a spectrum ripple of ~0.5 dB. Having the emitter side AR coated increases the FWHM and decreases the modulation ripple.

Figure 5 shows the relationship between the FWHM and the current injection to the $D_1$ electrode. The FWHM of the SLD varies linearly with increasing injection current. The resulting bandwidth is much broader than a typical QW SLD (i.e. 35 nm) at this wavelength with a short cavity in the gain section with uniform QWs [4]. The broad emission in our

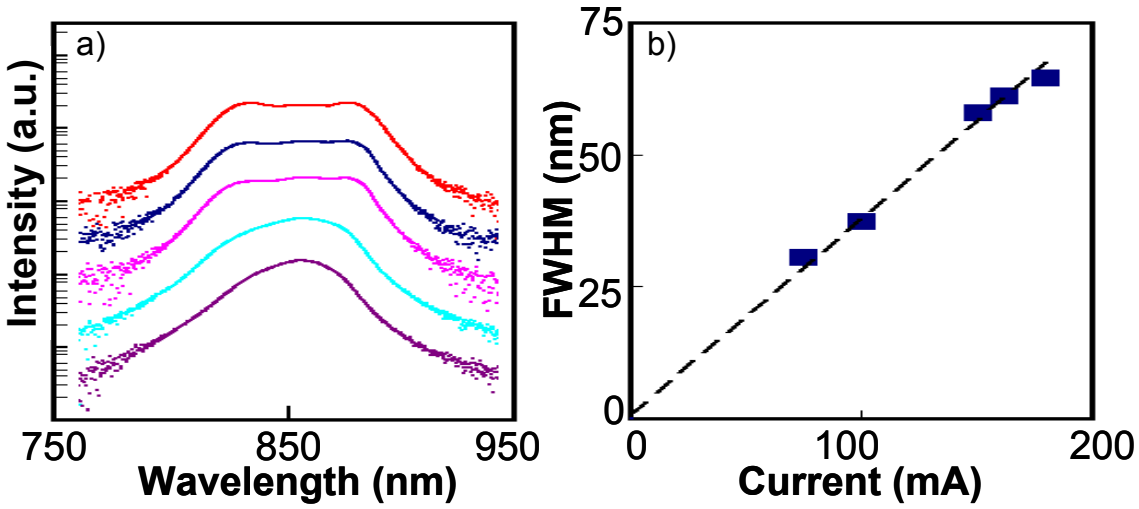


Fig. 4. a) Optical spectra acquired with a spectrum analyzer resolution of 2 nm for various injected currents to the $D_1$ section (which is 500 μm in length and AR coated) of the three-section SLD). b) The corresponding FWHM of an SLD with increasing injection current.

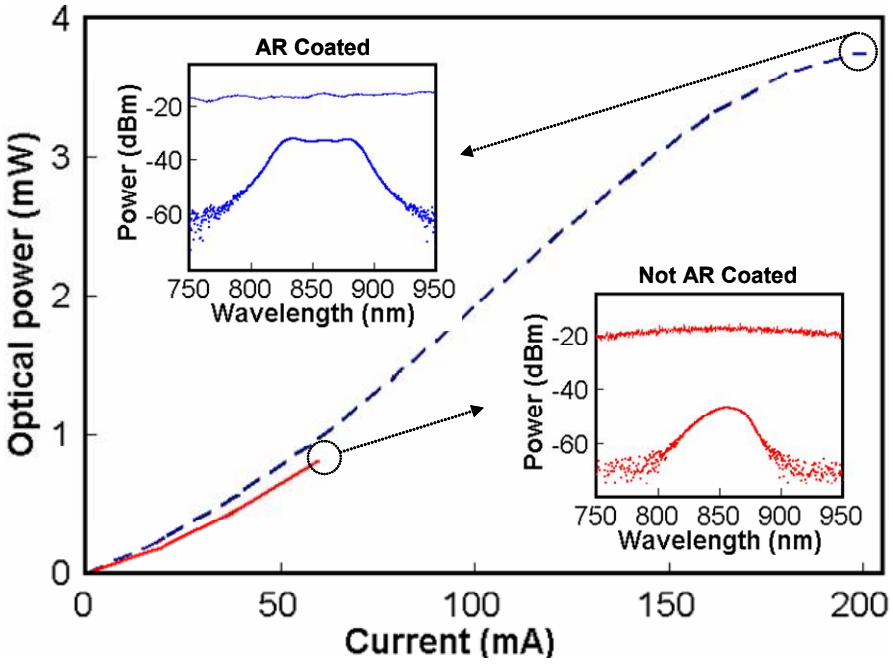


Fig. 3. The optical power versus total injection current to the $D_1$ section (500 μm) of the three-section SLD with and without AR coating on the emitter facet. The inset shows the corresponding spectrum and modulation for both devices measured using a spectrum analyzer with a resolution of 2 nm and 0.05 nm respectively.

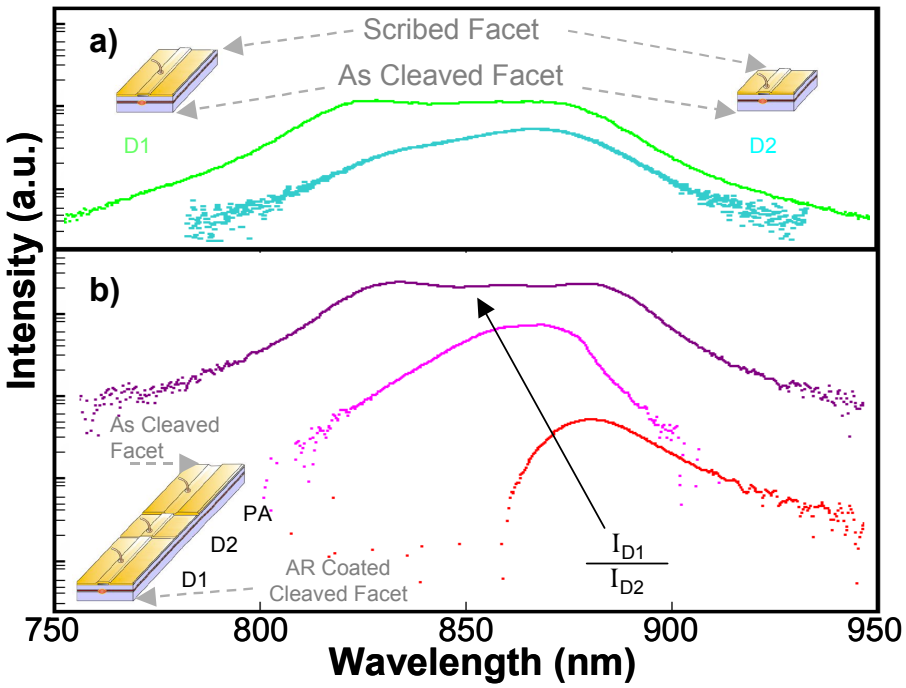


Fig. 6. The measured spectra from (a) a stand-alone gain section with scribed facets at a current injection of 200 mA and (b) three-section SLD with AR coating with varying current ratio of $D_1$(500 μm) to $D_2$.

device is associated with the simultaneous emission from ground and excited energy states. The SLD spectral behavior yields a coherence length of 5 μm with a FWHM of 65 nm and center wavelength of 850 nm.

In order to expound on the role of an integrated amplifier section and to confirm the simultaneous excitation of quantized states in QW's, we performed current excitation to $D_1$ with varying current injection. For comparison, stand-alone ridge devices are shown in Figure 6(a), consisting of only single ridge sections with an as-cleaved bare facet and a damaged (scribed) facet. Also depicted is the electroluminescent spectrum due to the spontaneous emission from such stand-alone $D_1$ (500 μm) and stand-alone $D_2$ (270 μm) sections under current injection of 200 mA. The maximum respective spectrum linewidth is 63 nm and 41 nm with a corresponding power of 1.8 mW and 1.5 mW and current at 190 mA and 160 mA. The challenge to manually damage a facet in a repeatable fashion resulted in a great deviation between devices in optical power and bandwidth by 1 mW and 15 nm respectively. The emission shows a high-energy shoulder at 835 nm and 870 nm from these broad spectra. The former hump is associated with the first excited state in the QW structure. This further corroborates the broad emission of our SLD earlier from the ground state and excited state emissions.

Fig. 6(b) presents the evolution (or reconfigurable injection scheme) of the three-section SLD spectrum with varying injected current ratio between gain to amplifier sections. The spectrum is progressively broadened and blue-shifted towards a shorter wavelength. At low injection level in $D_1$ ($I_{D1}/I_{D2}$~0.005, $I_{D2}$ = 200 mA), there is insufficient carrier density in the section and the gain section absorbs the emitted photons. This is especially the case at shorter wavelength regions, which results in similar bandgap energies to the absorber section. Therefore, the SLD emission with FWHM (30 nm) is dominated by the longer wavelength spontaneous emission from the ground state level, as the gain section absorbs the excited emission. Further increase in injected current at $D_1$ ($I_{D1}$ = $I_{D2}$ = 160 mA) results in a slight red shift in SLD spectrum with FWHM (29 nm). At a sufficiently moderate injection level at $D_2$ ($I_{D1}/I_{D2}$~200, $I_{D1}$ = 200 mA), $D_2$ section will be driven to transparent and operate as an optical amplifier. Stimulated emission in the gain medium of the amplifier $D_2$ causes amplification of incoming photon from gain section $D_1$ resulting in a broad spectrum emission, at almost twice the power of a stand-alone device (with a damaged absorber section).

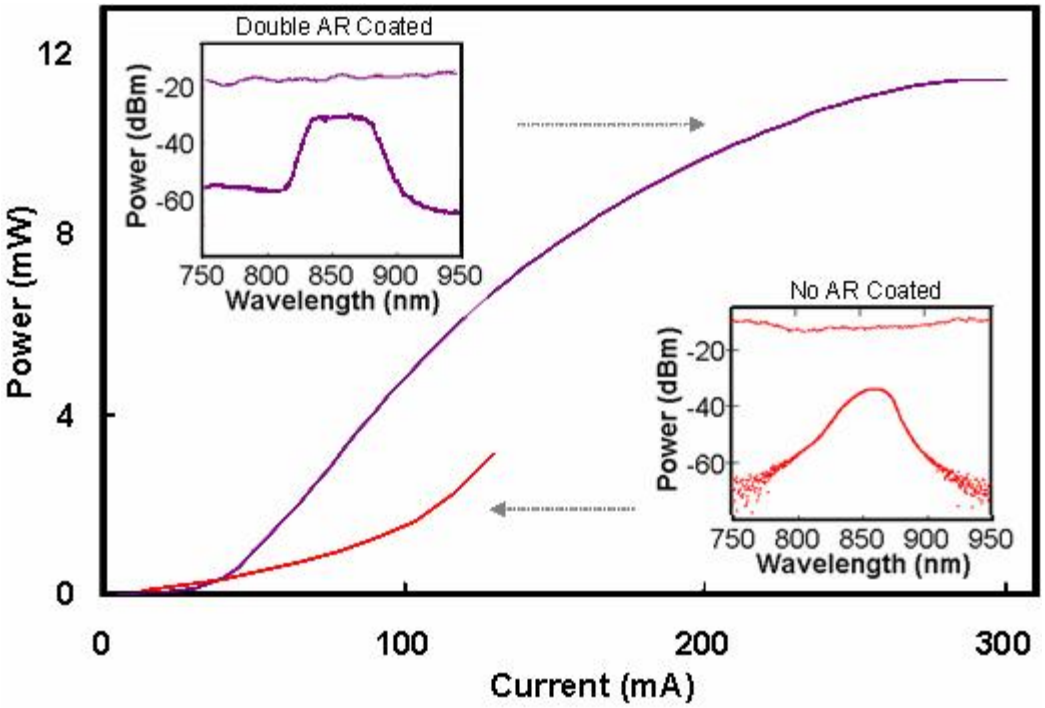


Fig. 7. The optical power versus total injection current to $D_1$ section (850 μm) of the three-section SLD with and without AR coating (on the emitter and absorber facet). The inset shows the corresponding spectrum and modulation for both

### 3.2 SLDs with $D_1$ at 850 μm Length

Devices with longer $D_1$ section for higher optical power operation were measured. Figure 7 shows the L-I characteristics of the SLD with $D_1$ 850 μm in length, before and after the application of AR coating to both facets (emitter and absorber). $D_1$ was driven with a CW current, while $D_2$ and PA were floating. The device with no AR coating exhibits lasing action at a current operation of 130 mA, yielding a bandwidth of 26 nm. With AR coating, a maximum output power exceeds 11 mW at a current injection of 200 mA. Above 200 mA of injection current, thermal roll off begins to appear, primarily due to the saturation in the gain section. The inset in Figure 7 presents the corresponding electroluminescent spectrum, centered at 850 nm, from SLDs with and without AR coating. Prior to entering the lasing regime, the spontaneous emission from the SLD without AR coating produces 2.1 mW of optical power with a FWHM of 36 nm and a spectral ripple of 0.6 dB. The AR-coated SLD produces a nearly flattop emission with a FWHM of 50 nm and a spectrum ripple of ~0.5 dB. Having both device facets AR coated increases the FWHM and decreases the modulation ripple.

The SLD spectral behavior yields a coherence length of 5 μm with a FWHM of 65 nm and center wavelength of 850 nm. The facet coating at the emitter side for this particular $D_1$ length resulted in a narrower bandwidth due to requiring a greater absorber length to suppress lasing. Since the $D_1$ cavity is longer than in the previous set of devices more current is needed to produce the same current density and emit the same optical power. Table I tabulates the results presented for both the 500 μm $D_1$ SLD and the 850 μm $D_1$ SLD.

| $D_1$ Length (μm) | AR Coating | $D_1$ Current (mA) | FWHM (nm) | Power (mW) | Ripple (dB) |
|---|---|---|---|---|---|
| 850 | Double sided | 200 | 50 | 11 | 0.5 |
| | None | 130 | 26 | 2.1 | 0.6 |
| 500 | Emitter only | 200 | 65 | 3.8 | 0.5 |
| | None | 60 | 33 | 0.8 | 0.6 |

Table 1. Summary table of optical characterization results of samples with various $D_1$ lengths and AR coatings.

## 4. CONCLUSION

In summary, we have characterized the three-section broadband GaAs/AlGaAs quantum-well based superluminescent diodes. The high power and broad emission spectrum from simultaneous emission of quantized states is attained by proper selection of device geometry and AR coating to allow the single current pumping source for photon generation in the gain section and for photon amplification in the amplifier section. A high power operation can be obtained from devices with longer $D_1$ section. The optimal integrated SLD device fabricated exhibits a FWHM of 65 nm, output power of 3 mW, and spectral ripple of 0.5 dB at wavelength center at 850 nm. This enables high resolution OCT imaging to be achieved.

## ACKNOWLEDGEMENTS

This work is supported in part by Carl Zeiss Meditec Inc. (Dublin, CA), and the Pennsylvania Infrastructure Technology Alliance (PITA), a partnership of Carnegie Mellon University, Lehigh University and the Commonwealth of Pennsylvania Department of Community and Economic Development.

## REFERENCES

1. M. E. Brezinski and J. G. Fujimoto, "Optical coherence tomography: high-resolution imaging in nontransparent tissue," IEEE. J. Select. Top. Quantum Electron., vol. 5, pp. 1185-1192, 1999.
2. B. Cense, N. A. Nassif, T. C. Chen, M. C. Pierce, S. H. Yun, B. H Park, B. E. Bouma, G. J. Tearney, and J. F. de Boer, "Ultrahigh-resolution high-speed retinal imaging using spectral domain optical coherence tomography," Opt. Exp., vol. 12, pp. 2435-2447, 2004.
3. A. E. Elsner, S. A. Burns, J. J. Weiter, and F. C. Delori, "Infrared imaging of sub-retinal structures in the human ocular fundus," Vision Res., vol. 36, pp. 191-205, 1996.
4. C. F. Lin and B. L. Lee, "Extremely broadband AlGaAs/GaAs superluminescent diodes," Appl. Phys. Lett., vol. 71, pp. 1598-1600, 1997.
5. C. E. Dimas, H. S. Djie and B. S. Ooi, "Superluminescent diodes using quantum dots superlattice," J. Cryst. Growth, vol. 288, pp. 153-156, 2006.
6. H. S. Djie, C. E. Dimas, and B. S. Ooi, "Wideband quantum-dash-in-well superluminescent diode at 1.6 μm," IEEE Photon. Technol. Lett., vol. 18, pp. 1747 – 1749, 2006.
7. M. L. Osowski, T. M. Cockerill, R. M. Lammert, D. V. Forbes, D. E. Ackley, and J. J. Coleman, "A strained layer InGaAs-GaAs-AlGaAs single quantum well broad spectrum LED by selective-area metalorganic chemical vapour deposition," IEEE Photon. Technol. Lett., vol. 6, pp. 1289-1291, 1994.

8. B. S. Ooi, K. McIlvaney, M. W. Street, A. Helmy, S.G. Ayling, A. C. Bryce, J. H. Marsh, and J. S. Roberts, "Selective quantum well intermixing in GaAs/AlGaAs structures using impurity-free vacancy diffusion," IEEE J. Quantum Electron., vol. 33, pp. 1784-1793, 1997.
9. A. T. Semenov, V. K. Batovrin, I. A. Garmash, V. R. Shidlovsku, M. V. Shramenko, and S. D. Yakubovich, "(GaAl)As SQW superluminescent diodes with extremely coherence length," Electron. Lett., vol. 31, pp. 315, 1995.
10. A.T. Semenov, V.R. Shidlovski, D.A. Jackson, R. Willsch, W. Ecke, "Spectral control in multisection AlGaAs SQW superluminescent diodesat 800 nm", Electron. Lett., vol. 32, pp 255-256, 1996
11. F. Causa, J. Sarma, "Realistic model for the output beam profile of stripe and tapered superluminescent light-emitting diodes", App. Opt., vol 42, Issue 21, pp. 4341-4348, 2003